Geochemistry Geophysics Geosystems G3
AN ELECTRONIC JOURNAL OF THE EARTH SCIENCES
Published by AGU and the Geochemical Society

Article
Volume 6, Number 8
10 August 2005
Q08003, doi:10.1029/2005GC000967
ISSN: 1525-2027

Deep mantle heat flow and thermal evolution of the Earth's core in thermochemical multiphase models of mantle convection

Takashi Nakagawa
Department of Earth and Planetary Sciences, University of Tokyo, Building #1, 7-3-1, Hongo, Bunkyo, Tokyo, 113-0033 Japan (takashi@eps.s.u-tokyo.ac.jp)

Paul J. Tackley
Department of Earth and Space Sciences, University of California, Los Angeles, 595 Charles Young Drive East, Los Angeles, California 90095, USA

Institute of Geophysics and Planetary Physics, University of California, Los Angeles, Los Angeles, California, USA

[1] A coupled model of thermochemical multiphase mantle convection and parameterized heat balance in the Earth's core is used to investigate the need for radioactive potassium in the core, and chemical layering above the core-mantle boundary (CMB), to obtain a successful thermal evolution of the core, i.e., one in which the magnetic field exists over geological time and the final inner core size matches that observed. The mantle convection model includes both the olivine and pyroxene phase change systems linked via the compositional field. The most successful core thermal evolution is obtained when the compositional density difference between subducted MORB and pyrolite in the deep mantle is 1.1% and the core contains 100 ppm radioactive potassium, both of which are consistent with estimates from laboratory experiments. In that scenario, the CMB heat flow at the present time is 8.5 TW, and the time-averaged ohmic dissipation is 2 TW. However, during the modeled magnetic evolution, the ohmic dissipation associated with the geodynamo occasionally becomes zero, which means that the geodynamo stops working, although these large fluctuations could be an artifact of two-dimensional geometry. Various model uncertainties still remain.

Components: 6470 words, 7 figures, 3 tables.

Keywords: core-mantle boundary; multicomponent phase changes; radioactive heating; thermal evolution.

Index Terms: 8115 Tectonophysics: Core processes (1213, 1507); 8124 Tectonophysics: Earth's interior: composition and state (1212, 7207, 7208, 8105); 8125 Tectonophysics: Evolution of the Earth (0325).

Received 10 March 2005; **Revised** 7 June 2005; **Accepted** 20 June 2005; **Published** 10 August 2005.

Nakagawa, T., and P. J. Tackley (2005), Deep mantle heat flow and thermal evolution of the Earth's core in thermochemical multiphase models of mantle convection, *Geochem. Geophys. Geosyst.*, *6*, Q08003, doi:10.1029/2005GC000967.

1. Introduction

[2] Explaining how the heat flux out of the core stayed large enough over billions of years to maintain the geodynamo without the inner core growing to a much larger size than observed is a challenging problem. Two proposed features that may aid in explaining this are (1) the presence of a dense chemically distinct layer above the core-mantle boundary (CMB), which reduces CMB heat flux and hence inner core growth and (2) the presence of radioactive potassium in the core [*Gessmann and Wood*, 2002; *Murthy et al.*, 2003; *Nimmo et al.*, 2004; *Labrosse*, 2003; *Lister*, 2003]. In our previous study [*Nakagawa and Tackley*, 2004a], a numerical thermochemical mantle convection calculation coupled to a parameterized core global heat balance model was used to investigate the first

mechanism, i.e., the influence of compositionally dense material on core and mantle thermal evolution. It was found that isochemical mantle convection results in a CMB heat flow that is too large, hence a too large inner core, while a globally continuous layer of dense material results in the CMB heat flow dropping to values that are too low to maintain the geodynamo. A successful core thermal evolution (i.e., one in which the geodynamo is powered over geological history and the present-day inner core is the observed size) was obtained only with a discontinuous layer of compositionally dense material above the CMB, which occurred when the density difference between pure "basalt" and hartzburgite in the deep mantle is about 2%. However, in that "successful" case the CMB heat flow was close to the lower limit of the predicted range required to drive the geodynamo [*Buffett*, 2002], suggesting that an additional mechanism, such as radioactive potassium in the core, might also be necessary.

[3] The effect of radioactive potassium in the core on thermal evolution has been investigated using models in which both the core and mantle are parameterized [*Labrosse*, 2003; *Nimmo et al.*, 2004], with the finding that at least 400 ppm of radioactive potassium is required to obtain a successful thermal evolution. However, this concentration is larger than the range predicted from laboratory experiments [*Murthy et al.*, 2003], which is 50 ppm to 250 ppm, suggesting that an additional mechanism, such as a reduction in CMB heat flow due to partial layering above the CMB, might also be necessary.

[4] Thus, as each mechanism is only marginally able to explain the core's thermal evolution per se, we here extend our previous model to study the thermal evolution where both mechanisms are present. Two additional improvements are also introduced: (1) a calculation of ohmic dissipation in the parameterized core model, in order to better determine when geodynamo action is possible, and (2) a treatment of both olivine and pyroxene-garnet system phase transitions, linked to the local composition.

[5] Regarding the magnetic evolution, theoretical models of the thermal evolution of Earth's core [*Labrosse*, 2003; *Buffett*, 2002; *Lister*, 2003] together with the scaling between ohmic dissipation and magnetic field strength inferred from numerical dynamo simulations [*Christensen and Tilgner*, 2004] have suggested that the ohmic dissipation ranges from 0.2 TW to O(1) TW. Regarding phase transitions, mantle convection models (including our previous core-mantle evolution study [*Nakagawa and Tackley*, 2004a]) typically include only the olivine-system transitions, even though the pyroxene-garnet system, which might constitute ~40% of mantle volume, undergoes a different set of transitions, both in depth of the transitions and density changes. Both systems have recently been incorporated into numerical mantle convection models [*Tackley and Xie*, 2003; *Xie and Tackley*, 2004a, 2004b], so we here include this treatment.

[6] In summary, we here use a numerical mantle convection model coupled to a parameterized core heat balance model to investigate the hypothesis that both radioactive potassium in Earth's core and a partial layer of chemically dense material above the CMB are required to explain the evolution of Earth's core and mantle, i.e., to facilitate geodynamo action over geological history without growing the inner core too large, while keeping the concentration of radioactive potassium within experimentally determined bounds. The tradeoff between the concentration of radioactive potassium in the core and the density anomaly of crustal material in the deep mantle is investigated, leading to the identification of viable evolution solutions, the most successful of which has radioactive potassium within experimental constraints. The CMB heat flow and ohmic dissipation for a successful scenario are estimated from theoretical studies.

2. Model

[7] The numerical code STAG3D is used to study thermochemical mantle convection in a two-dimensional half cylindrical shell [*Tackley and Xie*, 2003; *Xie and Tackley*, 2004a, 2004b] with the radii of the CMB and surface boundaries rescaled such that surface area ratios match those in spherical geometry [*van Keken*, 2001]. The compressible anelastic and infinite Prandtl approximations are made, as usual. The physical properties density, thermal expansivity, and thermal diffusivity are assumed to be dependent on depth, as in previous studies (e.g., plotted by *Tackley* [1998]).

[8] The viscosity is temperature-, depth- and yield stress-dependent given as

$$\begin{aligned} \eta_d(T,z) &= \eta_0[1+(\Delta\eta-1)H(0.7716-z)] \\ &\quad \cdot \exp[4.6(1-z)]\exp\left\lfloor\frac{27.631}{T+0.88}\right\rfloor \\ \sigma_Y(z) &= \sigma_b+\sigma_d(1-z) \\ \eta(T,z,\dot{e}) &= \min\left(\eta_d(T,z),\frac{\sigma_Y(z)}{2\dot{e}}\right) \end{aligned} \quad , \qquad (1)$$

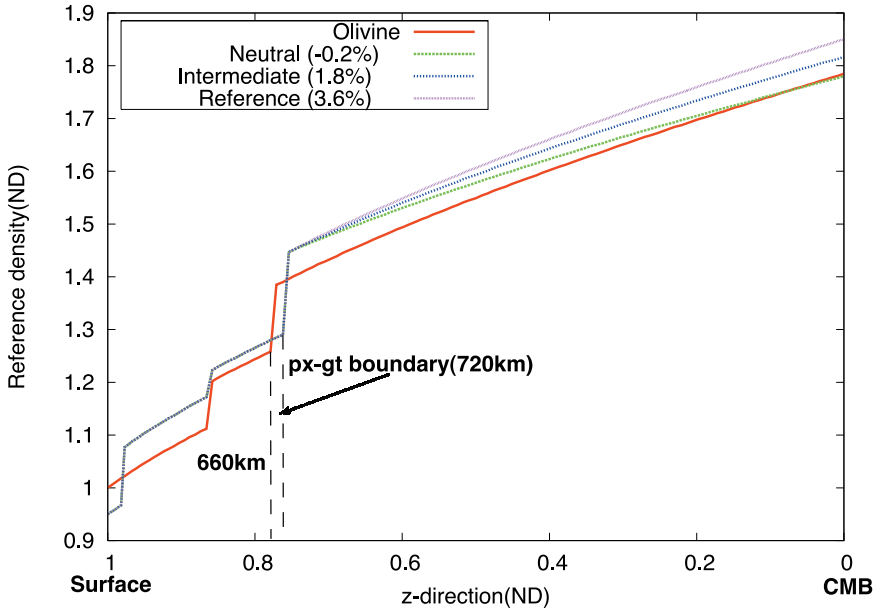

Figure 1. Reference density profiles for both phase change systems.

where $\eta_d(T, z)$ is the ductile viscosity, $\Delta\eta$ is the viscosity jump between upper and lower mantles, H is the Heaviside step function, $\sigma_Y(z)$ is the depth-dependent yield stress, σ_d is the yield stress gradient, σ_b is the yield stress at the surface, $\dot{e}$ is the second invariant of the strain rate tensor, and z is the vertical coordinate, which varies from 0 at the surface to 1 at the CMB. In this formulation, the viscosity changes by six orders of magnitude with temperature, two orders of magnitude with depth (though the increase along an adiabat is less), and $\Delta\eta = 10$ across the 660 km discontinuity.

[9] Compositional variations are assumed to arise from melt-induced differentiation, which is treated in the same manner as in previous studies [*Nakagawa and Tackley*, 2004a; *Xie and Tackley*, 2004a, 2004b], i.e., by comparing, after each time step, the local temperature to a depth-dependent solidus shown in Figure 1 of *Nakagawa and Tackley* [2004a]. When the temperature in a cell exceeds the solidus, the fraction of melt necessary to bring the temperature back to the solidus is generated and instantaneously placed at the surface to form crust, then the cell temperature is set back to the solidus [*Xie and Tackley*, 2004a]. Composition is represented by the variable C, which varies from 0 (harzburgite) to 1 (basalt/eclogite).

[10] The different phase changes in the olivine system and pyroxene-garnet system are implemented using the formulation described by *Xie and Tackley* [2004a], with parameters based on mineral physics data [*Irifune and Ringwood*, 1993; *Ono et al.*, 2001]. In this formulation there is one reference state for the olivine system and one for the pyroxene-garnet system, with physical properties in each cell obtained by linearly combining the properties of the two end-members, weighted by their fractions. Here we highlight only the two dynamically most important physical properties: density, which is also affected by thermal expansion, and effective thermal expansivity, which is affected by phase transitions as in [*Christensen and Yuen*, 1985]

$$\rho(T,z,f_{ol}) = \left[f_{ol}\bar{\rho}_{ol}(\bar{T},z) + (1-f_{ol})\bar{\rho}_{px}(\bar{T},z)\right] \cdot \left[1-\alpha_{eff}(T-\bar{T}(z))\Delta\rho_{th}\right], \quad (2)$$

$$\alpha_{eff} = \bar{\alpha}(z) + \sum_{i=1}^{nphase} f_i P_i \frac{d\Gamma_i}{dz}, \quad (3)$$

where $f_{ol} = 6/7(1 - C)$ is the olivine fraction, $\bar{\rho}(\overline{T}, z)$ is the reference density as a function of z and reference adiabatic temperature $\overline{T}(z)$ for both olivine and pyroxene systems, $\Delta\rho_{th}$ is the density variation due to the thermal effects, f_i is the fraction of the relevant component, P_i is the phase buoyancy parameter and Γ_i is the phase function for the ith phase change. The reference density profiles for both olivine and pyroxene-garnet systems are shown in Figure 1. The physical parameters associated with phase changes are listed in Table 1.

[11] Although the densities of the two systems are reasonably well known down to the top of the

Table 1. Physical Parameters for Multicomponent Phase Changes[a]

Number	Depth, km	Temperature, K	$\Delta\rho_{ph}$, kg m^{-3}	γ, MPa/K
Olivine-Spinel-Perovskite				
1	410	1600	280	+2.5
2	660	1900	400	−2.5
Pyroxene-Garnet-Perovskite				
1	60	0	350	0
2	400	1600	100	+1.0
3	720	1900	500	+1.0

[a] Taken from *Tackley and Xie* [2003]. The 60 km deep phase change in the pyroxene-garnet-perovskite system corresponds to the basalt-eclogite transition.

lower mantle, there is disagreement about the relative density at higher pressure due partly due to the effect of aluminum [*Weidner and Wang*, 1998], with some researchers suggesting a density crossover that would make MORB (predominantly the pyroxene component) less dense than pyrolite at CMB pressures [*Kesson et al.*, 1998; *Ono et al.*, 2001]. However, the most recent results suggest that MORB remains denser than pyrolite throughout the lower mantle [*Ono et al.*, 2005]. To explore the effect of this uncertainty we adopt three different values of the compressibility of the pyroxene-garnet component in the lower mantle, resulting in the density difference between pyroxene and olivine end-members at the CMB being −0.2% (here referred to as "neutral" because it is very close to zero compared to the other.), 1.8% (intermediate buoyancy) or 3.6% (reference buoyancy). Note that the "reference" buoyancy is so-called because the compressibility of the pyroxene system in the lower mantle is the same as that of the olivine system, not because it is preferred in any sense. The density contrast between actual mantle components is of course lower than this, for example, up to 2.16% between MORB (0% olivine) and pyrolite (60% olivine).

[12] Radioactive heating is included and is enhanced by a factor of ten in the dense material, to crudely account for the partitioning of incompatible heat-producing elements into the oceanic crust. Thus

$$R_h(C,t) = H_0\left(\frac{1+9C}{1+9\langle C\rangle}\right)\exp((t_a - t)\ln 2/\tau), \qquad (4)$$

where H_0 is the present-day heating rate in the regular mantle, t_a is the age of the Earth (4.5 Gyr), t is the time since the beginning of the calculation and τ is the average half-life of radiogenic heating, taken to be 2.43 Gyr. The averaged present-day internal heating rate in the mantle is set to 23.7 in the non-dimensional equations, corresponding to a dimensional value of 6.2×10^{-12} W/kg.

[13] The boundary conditions at the top and bottom boundaries are impermeable and shear stress free for velocity, isothermal for temperature and zero mass flux for composition. The side boundaries are periodic. The thermal boundary condition at the bottom boundary accounts for cooling of the core using the treatment of *Nakagawa and Tackley* [2004a], which is based on *Buffett et al.* [1992, 1996] and includes complexities associated with the inner core growth. In this study the calculation of ohmic dissipation is added, using the formulation from the theoretical study of *Lister* [2003]:

$$\Phi + (\varepsilon_L + \varepsilon_C)Q_R = (\varepsilon_S + \varepsilon_L + \varepsilon_C)F_{CMB} - \varepsilon_S F_{ad}, \qquad (5)$$

where Φ is the ohmic dissipation, F_{CMB} is the heat flow through the CMB calculated from the thermochemical multiphase mantle convection calculation, F_{ad} is heat flow through the CMB along a core adiabat, Q_R is the radioactive heating due to the potassium, and ε_s, ε_L and ε_C are the Carnot type efficiency for secular cooling, latent heat release and gravitational energy release, respectively. Q_R is given as

$$Q_R = \frac{4}{3}\pi\rho_c\left(r_{CMB}^3 - r_{IC}^3\right)H_K C_K \exp\left[\lambda_K\left(t_{age} - t\right)\right], \qquad (6)$$

where $H_K = 3.45 \times 10^{-9}$ W/kg is the heating rate per unit mass of potassium, C_K is a concentration of radioactive potassium in the outer core, which is varied from 0 ppm to 400 ppm, and $\lambda_K = 2.41 \times 10^{-10}$ yr^{-1} is the decay constant.

[14] A numerical grid of 256 (horizontal) × 64 (vertical) cells is used, with an average of 16 tracers per grid cell to track the composition. Physical parameters for the mantle are listed in Table 2, while parameters used in the global heat balance in the core are listed in Table 3.

[15] Cases are started from an initial condition in which the temperature field is adiabatic (potential temperature 1800 K) with thin error function thermal boundary layers at top and bottom plus small random perturbations, and the compositional field is initialized at a constant C = 0.3 (C = 0 corresponds to harzburgitic material with a 6:1 ratio of olivine to pyroxene and C = 1 corresponds to basaltic material with 100% pyroxene). The temperature at the CMB is initialized at 4200K,

Table 2. Mantle Model Physical Mantle Parameters[a]

Symbol	Meaning	Non-D. Value	Dimensional Value
Ra_0	Rayleigh number	10^7	N/A
η_0	reference viscosity	1	1.4×10^{22} Pa s
$\Delta\eta$	viscosity jump at 660 km	10	N/A
σ_b	yield stress at surface	1×10^5	117 MPa
σ_d	yield stress gradient	4×10^5	162.4 Pa m^{-1}
ρ_0	reference (surface) density	1	3300 kg m^{-3}
g	gravity	1	9.8 m s^{-2}
α_0	ref. (surface) thermal expan.	1	5×10^{-5} K^{-1}
κ_0	ref. (surface) thermal diff.	1	7×10^{-7} m^2 s^{-1}
ΔT_{sa}	temperature scale	1	2500 K
T_s	surface temperature	0.12	300 K
L_m	latent heat	0.2	6.25×10^5 J kg^{-1}
τ	half-life	0.00642	2.43 Gyr

[a] $Ra_0 = \rho_0 g \alpha_0 \Delta T_{sa} d^3 / \kappa_0 \eta_0$.

corresponding to the solidus temperature of a pyrolite composition at CMB [*Boehler*, 2000].

3. Results

3.1. Experimental Details

[16] Six values for the concentration of radioactive potassium in the core (0 ppm, 50 ppm, 100 ppm, 200 ppm, 250 ppm and 400 ppm) are tried for each of the three values of compositional density variation in the deep mantle, resulting in a total of 18 cases. Time integrations are started at t = 0 Gyr and run to the present-day t = 4.5 Gyr, corresponding to 0.0118 non-dimensional units. In order for a case to be judged successful, its final inner core radius must be similar to Earth's, i.e., 1220 km and its ohmic dissipation must remain high enough for a geodynamo to exist.

3.2. Thermochemical Structures and Time Diagnostics With No Core Potassium

[17] The final temperature and compositional fields for each density variation and with no potassium in the core are shown in Figure 2. In the neutral deep-mantle density contrast case (hereafter referred to as "neutral buoyancy case"), there is no chemical layering above the CMB; strips of subducted crust and residue exist throughout the mantle. In the intermediate buoyancy case, a large dense pile is found above the CMB in one place but cold subducted slabs can reach the CMB elsewhere. In the reference buoyancy case, a globally continuous, quite thick layer forms above the CMB. This layer deflects subducted slabs. In all cases, some compositional stratification is observed between the upper and lower mantles because of the density inversion between the olivine and pyroxene components that occurs between 660 km and 720 km, as also found previously [*Xie and Tackley*, 2004a, 2004b; *Ogawa*, 2003].

[18] The time variation of CMB heat flow, inner core size, ohmic dissipation and surface heat flow is plotted in Figure 3. Whereas the CMB heat flow is always positive in the neutral buoyancy case, it drops to approximately zero several times in the intermediate buoyancy case, and becomes negative in the reference buoyancy case. This is due to the

Table 3. Physical Parameters for the Core Heat Balance[a]

Symbol	Meaning	Value
r_{CMB}	radius of the core	3486 km
ρ_c	init. density of core	12300 kg m^{-3}
ρ_{iron}	density of pure iron	12700 kg m^{-3}
ρ_{li}	density of light elements	4950 kg m^{-3}
$\Delta\rho_{IC}$	density difference	400 kg m^{-3}
ΔS	entropy change	118 J kg^{-1} K^{-1}
$C_l(t = 0)$	init. cont. of light elements	0.035
C_c	heat capacity of the core	800 J kg^{-1} K^{-1}
$T_L(r = 0, C_l(t = 0))$	melting temp. at the center	5300K

[a] The value of entropy change is taken from *Labrosse et al.* [2001]. The melting temperature at the Earth's center is taken from *Lister* [2003]. All other values are taken from *Buffett et al.* [1996].

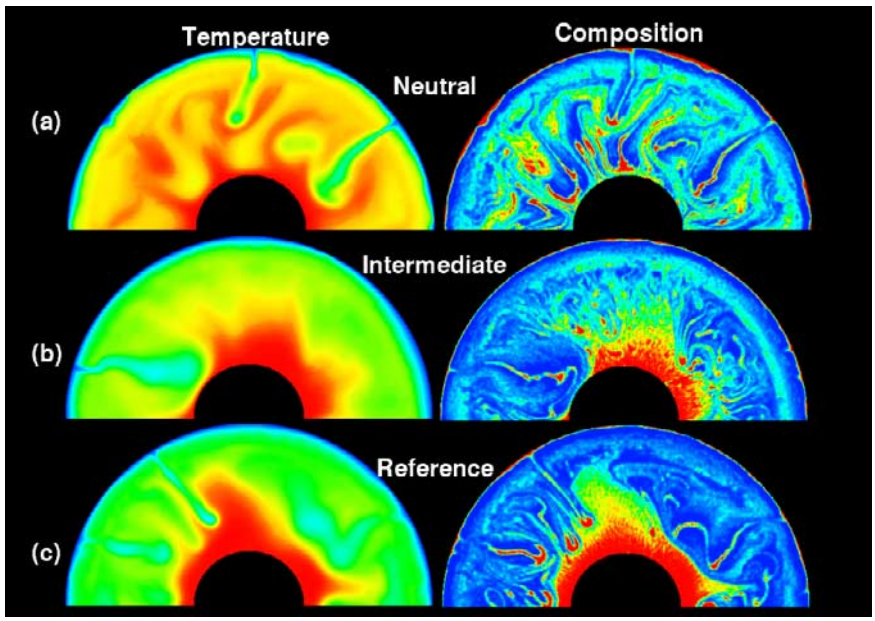

Figure 2. Temperature and compositional fields for all density models for cases with no potassium in the core. (a) Neutral buoyancy. (b) Intermediate buoyancy. (c) Reference buoyancy. Red indicates hot temperature and basaltic material. Blue indicates cold temperature and hartzburgite composition.

blanketing of the core with dense material that becomes as hot or hotter than the core due to its enrichment in heat-producing elements. The neutral and intermediate cases have a present-day core heat flow of 5 and 6.5 TW, respectively. Ohmic dissipation displays similar trends but becomes zero for short periods of time in the intermediate buoyancy case due to CMB heat flow being less than that conducted down the core adiabatic. Note that it is not physically meaningful to have negative dissi-

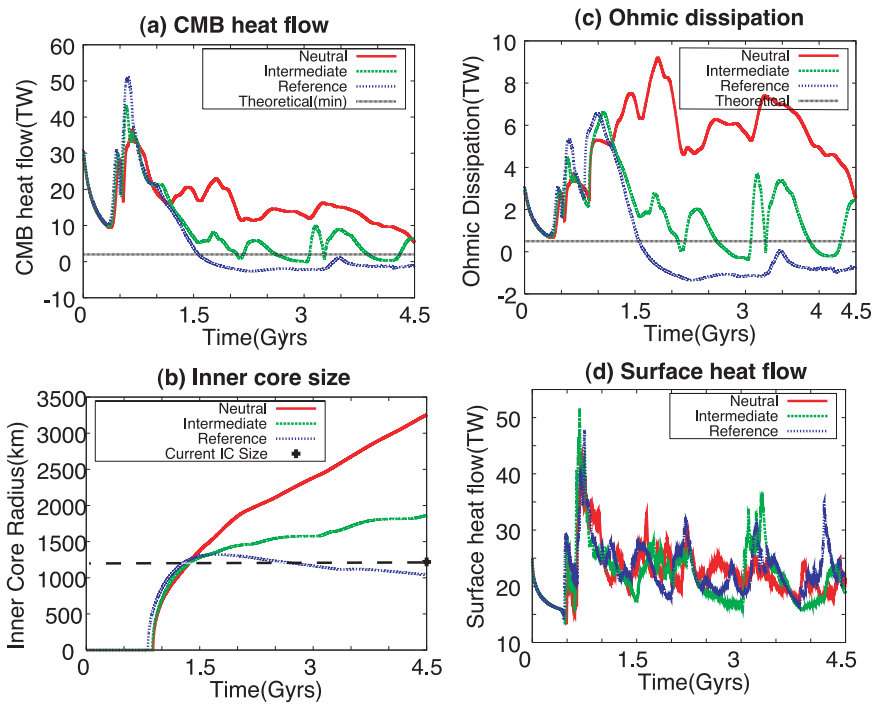

Figure 3. Time series of (a) CMB heat flow, (b) inner core size, (c) ohmic dissipation, and (d) surface heat flow in cases with no potassium in the core. Theoretical values for minimum CMB heat flow and ohmic dissipation are taken from *Buffett* [2002], which are 2 TW and 0.5 TW, respectively.

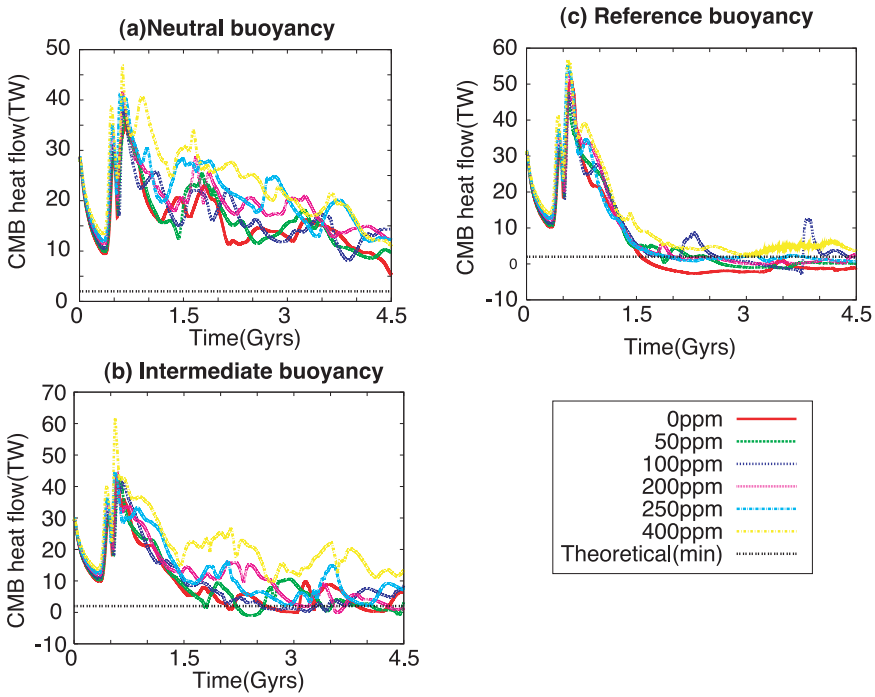

Figure 4. Time series of CMB heat flow for cases with various amount of radioactive potassium in the core. (a) Neutral buoyancy. (b) Intermediate buoyancy. (c) Reference buoyancy.

pation; when the curve drops to zero it simply indicates there is no convection or dynamo in the core. The present-day dissipation in the neutral and intermediate cases is around 2.5 TW. In the high buoyancy case, there is no geodynamo after about 1.5 Gyr into the calculation.

[19] The inner core size (Figure 3b) becomes much too large in both neutral and intermediate cases, whereas for the reference case it is close to, but slightly smaller than, the correct value. The surface heat flow (Figure 3d) has a present-day value of around 20 TW for all cases, which is a factor of two lower than the observationally constrained value of 44 TW [*Pollack et al.*, 1993], due partly to the absence of heat-producing elements in continental crust, and perhaps also due to the absence of supercontinent cycles, which may cause a strong episodicity in the flux [*Grigné et al.*, 2005].

[20] In summary, a satisfactory thermal evolution is not obtained in these cases: either the inner core becomes too large (neutral and intermediate cases) or the geodynamo dies out (reference and sometimes intermediate cases).

3.3. CMB Heat Flow

[21] Figure 4 shows the time evolution of the CMB heat flow for all cases. With neutral buoyancy (Figure 4a), the CMB heat flow is not strongly affected by the concentration of potassium in the core, with higher concentrations leading to higher heat flow on average, but with large fluctuations. Values at the present time range from 5 to 15 TW. For the intermediate buoyancy cases (Figure 4b), the CMB heat flow sometimes drops close to zero with 0 ppm potassium as previously discussed, but increases significantly as more K is added, staying above 10 TW with the highest concentration (400 ppm). Indeed, the 400 ppm case has a similar evolution to the neutral buoyancy cases, illustrating the effectiveness of core radioactive heating in keeping the CMB temperature high. The present-day CMB heat flow ranges from ~1 TW to 13 TW. For the reference buoyancy cases (Figure 4c), the CMB heat flow is very low from about 1.5 Gyr into the calculations due to the CMB becoming surrounded by hot dense material. Only with 250 or 400 ppm does it remain above zero at all times. The present-day CMB heat flow ranges from ~4 TW to negative.

3.4. Inner Core Size

[22] Figure 5 shows the time evolution of the inner core size for all cases. In all "neutral" cases (Figure 5a), the inner core grows to a larger size than observed, even with 400 ppm

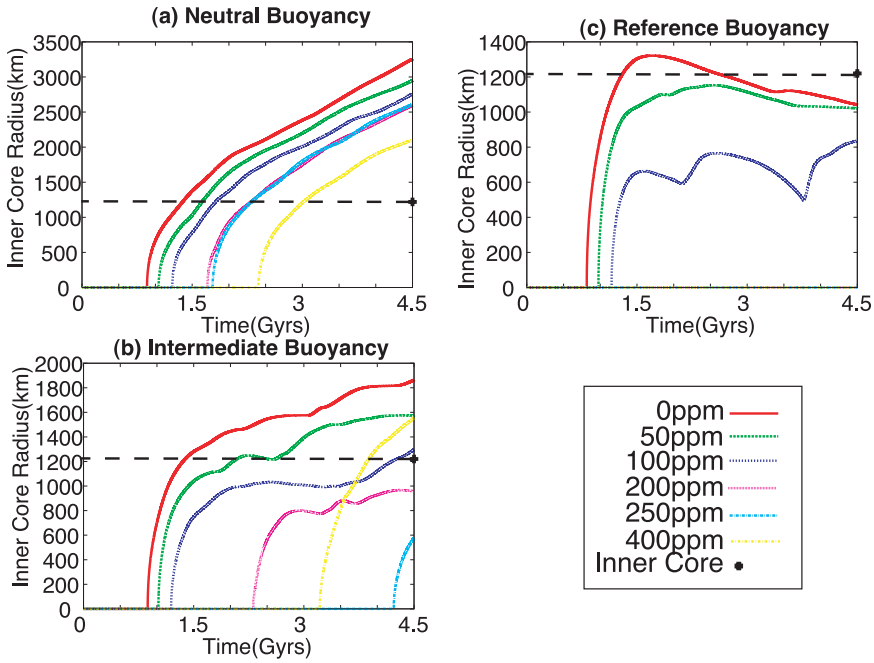

Figure 5. Time series of inner core size for cases with various amount of radioactive potassium in the core. (a) Neutral buoyancy. (b) Intermediate buoyancy. (c) Reference buoyancy.

potassium, the preferred amount of radioactive potassium in the parameterized model of *Nimmo et al.* [2004]. For intermediate buoyancy (Figure 5b), a reasonable inner core size is obtained with a K concentration between 100 ppm and 200 ppm. The onset time of the inner core in these models ranges from 1.2 Gyr to 2.3 Gyr, giving a relatively old inner core compared to predictions from completely parameterized models, in which the onset time of inner core growth is estimated to be ~3 Gyr, giving an inner core only 1.5 Gyr old [*Labrosse et al.*, 2001; *Nimmo et al.*, 2004]. With the reference buoyancy (Figure 5c), the final inner core size is less than observed for all cases, and for more than 200 ppm, the inner core does not appear at all.

3.5. Ohmic Dissipation

[23] Figure 6 shows the time evolution of ohmic dissipation for all cases. In all of the neutral cases (Figure 6a), the ohmic dissipation is at least ~1 TW and typically several TW at all times (present-day 2.5–6.5 TW), indicating the continuous presence of a magnetic field. In the intermediate cases (Figure 6b), the dissipation sometimes drops to zero in all except for 400 ppm case, implying that the geodynamo temporarily stops several times, although present-day values range from about ~1 to 3.5 TW. In the reference cases (Figure 6c), all cases display long periods of zero ohmic dissipation after about 1.5 Gyr.

3.6. Regime Diagram

[24] It has previously been found that fluctuations in globally averaged quantities such as mass flux or heat flux are much larger in 2-D calculations than in similar 3-D calculations [e.g., *Tackley et al.*, 1994; *Tackley*, 1997]; thus the fluctuations in CMB heat flux and dissipation obtained here are likely much larger than realistic, although it remains to be established by how much. For this reason, it seems appropriate to consider the dissipation averaged over some suitable time interval, rather than the dissipation at every moment in time, when estimating whether dynamo action can be driven. As all models maintain positive dissipation during the first ~1.5 Gyr, we here consider the dissipation averaged over the last 3 Gyr, and plot this versus final core radius for all cases so that the tradeoffs between the two varied input parameters (deep mantle density contrast and core K content) are clearly visible (Figure 7). The dashed lines in Figure 7 indicate the current core size (red) and zero ohmic dissipation (black). Values of less than zero are not physically meaningful but should be taken to indicate that the model has failed to maintain a geodynamo.

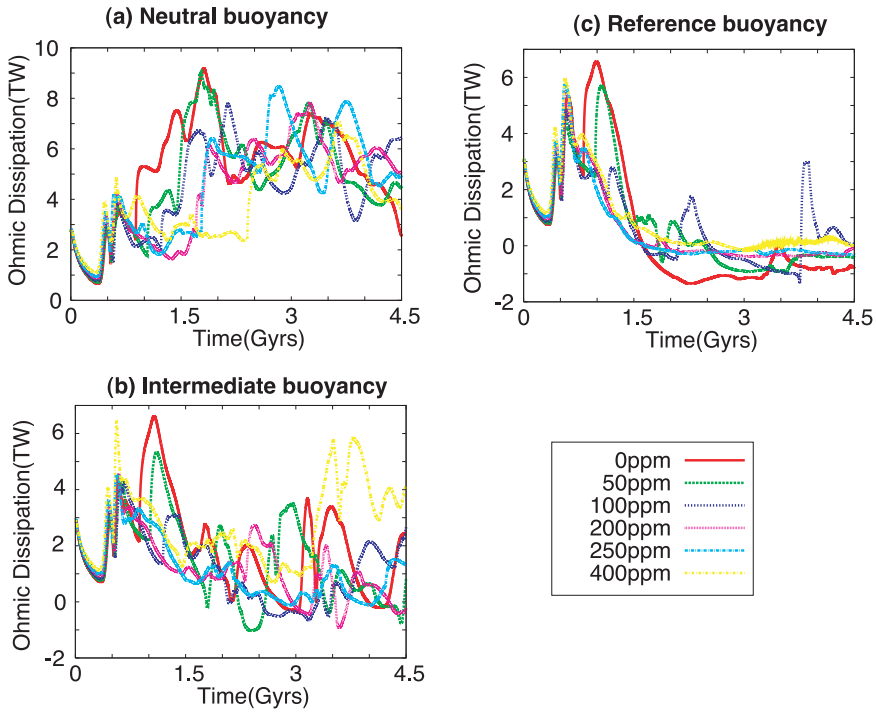

Figure 6. Time series of ohmic dissipation for cases with various amount of radioactive potassium in the core. (a) Neutral buoyancy. (b) Intermediate buoyancy. (c) Reference buoyancy.

[25] The three groups of points in Figure 7 representing the three different deep mantle density contrasts show a clear, almost linear trend, with both of the two varied input parameters affecting the results in a similar manner. Specifically, increasing K core content results in lower ohmic dissipation and a smaller inner core, and so does increasing the density contrast of subducted basalt. However, while the trends are qualitatively similar, their slopes in dissipation-core size space are different, with changing K causing less difference to the ohmic dissipation for a given change in inner core size, than changing the basalt density contrast. Thus the points for intermediate and reference buoyancies overlap with respect to inner core size, but are distinctly different with respect to ohmic dissipation.

[26] Neutral buoyancy cases all have a too-large inner core, even with large concentrations of radioactive K. It is likely that larger concentrations would eventually bring the inner core size into the correct range, but 400 ppm is already larger than experimental constraints allow. Reference buoyancy cases all have too low ohmic dissipation, such that a geodynamo would not operate. Intermediate buoyancy is needed for a successful evolution. The best agreement for both quantities is obtained when the concentration of core potassium is around 100 ppm and the compositional density variation at the CMB is 1.8%. This value of compositional density difference is consistent with our previous result using a single-component phase change system [*Nakagawa and Tackley*, 2004a]. This concentration of radioactive potassium is consistent with the constraint from laboratory experiments [*Murthy et al.*, 2003]. In this case, the CMB heat flow at the present time is 8.5 TW, which is consistent with theoretical estimates of the CMB heat flow [*Buffett*, 2002]. A concern, how-

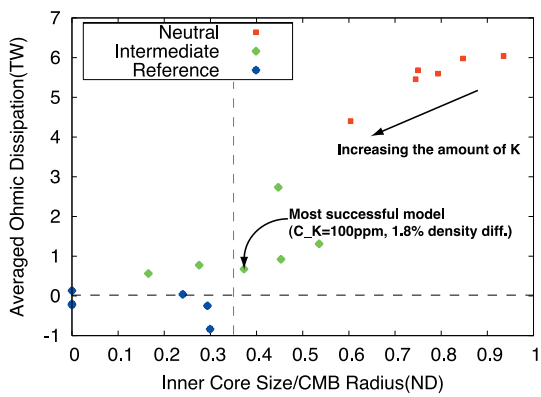

Figure 7. Summary diagram showing ohmic dissipation (averaged over the last 3 Gyr) versus present-day inner core size, for all cases.

ever, is that the ohmic dissipation (Figure 6b) does reach zero several times, but as argued earlier, these large fluctuations about the time-averaged value may be an artifact of using 2-D geometry. If we were to take finer steps in (density contrast, [K]) space then other combinations may result in a successful evolution, most likely with one parameter higher and the other parameter lower.

4. Discussion: Model Uncertainties

[27] Various approximations or uncertainties in the model may affect the results and should be investigated in the future. The main uncertainties, as already discussed, are the chemical density variation in the deep mantle and the concentration of radioactive K in the core, which we have thus varied.

[28] For the mantle model, the main approximations (roughly order of likely importance) are as follows:

[29] 1. Rheology: This is greatly simplified, partly because it is desirable to study simple cases first. The viscosity variation with temperature is substantially reduced relative to realistic values. Physically, this reduces the self-regulation of mantle temperature [*Tozer*, 1972], which is thought to be important for thermal evolution, and also results in slabs being less stiff than realistic and plumes being less weak than realistic. The effect of water, which has been proposed to have a strong influence on heat transport by mantle convection [*Korenaga*, 2003], and viscoelasticity, which is likely important in the plate tectonic process, are also neglected.

[30] 2. Geometry: The influences of three-dimensional spherical shell geometry need to be investigated, because the convective planform of thermochemical convection is inherently three-dimensional [e.g., *Tackley*, 1998; *McNamara and Zhong*, 2004]. *Stegman et al.* [2003] applied a 3-D spherical thermochemical convection model with a parameterized core to study Moon evolution. Recently heat transfer for layered 3-D spherical convection was studied [*Oldham and Davies*, 2004], but their model used simple time-independent heating and the heat flow through the CMB ranged from 1 TW to 4 TW- at the low end of maintaining the geodynamo, because the convective vigor in that model is lower than the realistic.

[31] 3. Continents: These have several possible effects on heat transport by mantle convection. The continental crust contains high concentrations of radioactive heat-producing elements, and also continents may reduce mantle heat loss through a thermal blanketing effect [*Grigné and Labrosse*, 2001], although it has also been proposed that continents increase mantle heat loss [*Lenardic et al.*, 2005]. Furthermore, continents influence the style of mantle convection and may induce an episodicity in global heat transport [*Grigné et al.*, 2005].

[32] 4. The perovskite-postperovskite phase change: This newly discovered transition [*Murakami et al.*, 2004; *Oganov and Ono*, 2004; *Tsuchiya et al.*, 2004] has been shown to increase CMB heat flow [*Nakagawa and Tackley*, 2004b] and destabilize chemical layering [*Nakagawa and Tackley*, 2005] and should thus be included in future evolution studies. In order to obtain observed "double crossing" features found in the Caribbean and Eurasia regions [*Thomas et al.*, 2004a, 2004b], *Hernlund et al.* [2005] estimated that the CMB temperature is in the range 4000 to 4200 K. However, with the present core parameterization this would lead to a too small inner core.

[33] 5. Mantle properties such as the concentration of heat-producing elements (particularly in the crustal material) and thermal conductivity, for which pressure and temperature dependence may be important [*Hofmeister*, 1999].

[34] 6. The initial condition for the mantle, both thermal and compositional: This may also be important, but for the compositional initial condition, our previous study [*Nakagawa and Tackley*, 2004a] has already been checked between layered and homogeneous start and not affected very much.

[35] Some additional uncertainties in the core parameterization are (1) the melting temperature at the center of the Earth, estimates of which range from 4800 K to 5800 K or hotter [*Alfe et al.*, 2002], (2) the initial temperature of the core (CMB), and (3) the scaling between the ohmic dissipation and magnetic field strength, which has been challenged using results from a numerical dynamo model [*Christensen and Tilgner*, 2004], which, however, itself has various uncertainties.

5. Summary and Conclusions

[36] A numerical model of thermochemical multiphase mantle convection coupled to a parameterized global heat balance model was used to investigate the effect of two major uncertain

parameters on the thermal evolution of the core and determine which combination(s) lead to a successful thermal evolution. The two parameters are the density contrast of subducted MORB in the deep mantle, and the concentration of radioactive potassium in the core. The major findings are as follows:

[37] 1. Increasing [K] and increasing density contrast both lead to lower time-averaged ohmic dissipation and a smaller inner core, but chemical density contrast has the stronger effect on ohmic dissipation.

[38] 2. Both potassium in the core, and a partial layer of segregated former oceanic crust above the CMB, are necessary to obtain an evolution in which the geodynamo exists over geological time and the inner core is the correct size with a reasonable [K], at least with the present model approximations.

[39] 3. In the most successful model, (1) the concentration of radioactive K is 100 ppm, which is within the experimentally determined range of 50 to 250 ppm [*Murthy et al.*, 2003], (2) the density difference between the pyroxene and olivine end-members in the deep mantle is 1.8%, corresponding to a difference between MORB and pyrolite of 1.1%, within the range estimated from recent laboratory results [*Ono et al.*, 2005], (3) the CMB heat flow is around 8.5 TW, which is consistent with theoretical estimates [*Buffett*, 2002], (4) the age of the inner core is over 3 Gyr, which is old compared to parameterized models [*Labrosse et al.*, 2001; *Nimmo et al.*, 2004], (5) ohmic dissipation over the last 3 Gyr is of O(1) TW but drops to zero at several points in the calculation; it is thought that this is due to unrealistically large fluctuations that are artifact of using only 2-D geometry, but this must be verified in future.

[40] In future the effect of first-order model approximations (simplified rheology and geometry), as well as additional physical complexities such as the postperovskite phase transition, must be determined. The sensitivity of the thermal evolution to uncertainties in core melting temperature and initial CMB and mantle temperatures must also be evaluated. The effect of amount of enhancement of radiogenic heat sources in the basaltic material should also be checked. In order to fully understand mantle thermochemical evolution, trace element isotopes must be tracked as in some recent models [*Xie and Tackley*, 2004a, 2004b]; but those models assumed a very simple ''constant heat capacity'' core parameterization and should be further developed using a more realistic treatment of the core as well as using fewer approximations as discussed earlier.

Acknowledgments

[41] T.N. is financially supported by the 21st Century COE program for Earth Sciences, University of Tokyo, and P.J.T. is supported by NSF grant EAR0207741. Bruce Buffett and Stephane Labrosse gave us constructive comments and discussions regarding the core cooling model. The authors thank Magali Billen, Allen K. McNamara, and an anonymous reviewer for constitutive reviews.

References

Alfe, D., M. J. Gillan, and D. G. Price (2002), Composition and temperature of the Earth's core constrained by ab initio calculations and seismic data, *Earth Planet. Sci. Lett.*, *195*, 91–98.

Boehler, R. (2000), High-pressure experiments and the phase diagram of lower mantle and core material, *Rev. Geophys.*, *38*, 221–245.

Buffett, B. A. (2002), Estimates of heat flow in the deep mantle based on the power requirements for the geodynamo, *Geophys. Res. Lett.*, *29*(12), 1566, doi:10.1029/2001GL014649.

Buffett, B. A., H. E. Huppert, J. R. Lister, and A. W. Woods (1992), Analytical model for solidification of the Earth's core, *Nature*, *356*, 329–331.

Buffett, B. A., H. E. Huppert, J. R. Lister, and A. W. Woods (1996), On the thermal evolution of the Earth's core, *J. Geophys. Res.*, *101*, 7989–8006.

Christensen, U. R., and A. Tilgner (2004), Power requirement of the geodynamo from ohmic losses in numerical and laboratory dynamos, *Nature*, *429*, 169–171.

Christensen, U. R., and D. A. Yuen (1985), Layered convection induced by phase transitions, *J. Geophys. Res.*, *90*, 291–300.

Gessmann, C. L., and B. J. Wood (2002), Potassium in the Earth's core, *Earth Planet. Sci. Lett.*, *200*, 63–78.

Grigné, C., and S. Labrosse (2001), Effects of continents on earth cooling: Thermal blanketing and depletion in radioactive elements, *Geophys. Res. Lett.*, *28*, 2707–2710.

Grigné, C., S. Labrosse, and P. J. Tackley (2005), Convective heat transfer as a function of wavelength: Implications for the cooling of the Earth, *J. Geophys. Res.*, *110*, B03409, doi:10.1029/2004JB003376.

Hernlund, J. W., C. Thomas, and P. J. Tackley (2005), A doubling of the post-perovskite phase boundary and structure of the Earth's lowermost mantle, *Nature*, *434*, 882–886.

Hofmeister, A. M. (1999), Mantle values of thermal conductivity and the geotherm from phonon lifetimes, *Science*, *283*, 1699–1706.

Irifune, T., and A. E. Ringwood (1993), Phase transformations in subducted oceanic crust and buoyancy relationship at depths of 600–800 km in the mantle, *Earth Planet. Sci. Lett.*, *117*, 101–110.

Kesson, S. E., J. D. F. Gerald, and J. M. Shelley (1998), Mineralogy and dynamics of a pyrolite lower mantle, *Nature*, *393*, 252–255.

Korenaga, J. (2003), Energetics of mantle convection and the fate of fossil heat, *Geophys. Res. Lett.*, *30*(8), 1437, doi:10.1029/2003GL016982.

Labrosse, S. (2003), Thermal and magnetic evolution of the Earth's core, *Phys. Earth Planet. Inter.*, *140*, 127–143.

Labrosse, S., J.-P. Poirier, and J.-L. Mouel (2001), The age of the inner core, *Earth Planet. Sci. Lett.*, *190*, 111–123.

Lenardic, A., L. N. Moresi, A. M. Jellinek, and M. Manga (2005), Continental insulation, mantle cooling, and the surface area of oceans and continents, *Earth Planet. Sci. Lett.*, *234*, 317–333.

Lister, J. R. (2003), Expression for the dissipation driven by convection in the Earth's core, *Phys. Earth Planet. Inter.*, *140*, 145–158.

McNamara, A. K., and S. Zhong (2004), The influence of thermochemical convection on the fixity of mantle plumes, *Earth Planet. Sci. Lett.*, *222*, 485–500.

Murakami, M., K. Hirose, N. Sata, Y. Ohishi, and K. Kawamura (2004), Phase transition of $MgSiO_3$ perovskite in the deep lower mantle, *Science*, 855–858.

Murthy, V. R., W. van Westrenen, and Y. Fei (2003), Radioactive heat source in planetary cores: Experimental evidence for potassium, *Nature*, *423*, 164–165.

Nakagawa, T., and P. J. Tackley (2004a), Effects of thermochemical mantle convection on the thermal evolution of the Earth's core, *Earth Planet. Sci. Lett.*, *220*, 107–119.

Nakagawa, T., and P. J. Tackley (2004b), Effects of a perovskite-post perovskite phase change near core-mantle boundary in compressible mantle convection, *Geophys. Res. Lett.*, *31*, L16611, doi:10.1029/2004GL020648.

Nakagawa, T., and P. J. Tackley (2005), The interaction between the post-perovskite phase change and a thermochemical boundary layer near the core-mantle boundary, *Earth Planet. Sci. Lett.*, in press.

Nimmo, F., G. D. Price, J. Brodholt, and D. Gubbins (2004), The influence of potassium on core and geodynamo evolution, *Geophys. J. Int.*, *156*, 363–376.

Oganov, A. R., and S. Ono (2004), Theoretical and experimental evidence for a post-perovskite phase of $MgSiO_3$ in Earth's D″ layer, *Nature*, *430*, 445–448.

Ogawa, M. (2003), Chemical stratification in a two-dimensional convecting mantle with magmatism and moving plates, *J. Geophys. Res.*, *108*(B12), 2561, doi:10.1029/2002JB002205.

Oldham, D., and J. H. Davies (2004), Numerical investigation of layered convection in a three-dimensional shell with application to planetary mantles, *Geochem. Geophys. Geosyst.*, *5*, Q12C04, doi:10.1029/2003GC000603.

Ono, S., E. Ito, and T. Katsura (2001), Mineralogy of subducted basaltic crust (MORB) from 25 to 37 GPa, and chemical heterogeneity of the lower mantle, *Earth Planet. Sci. Lett.*, *190*, 57–63.

Ono, S., Y. Ohishi, M. Isshiki, and T. Watanuki (2005), In situ X-ray observations of phase assemblages in peridotite and basalt compositions at lower mantle conditions: Implications for density of subducted oceanic plate, *J. Geophys. Res.*, *110*, B02208, doi:10.1029/2004JB003196.

Pollack, H. N., S. J. Hunter, and R. Johnston (1993), Heat loss from the Earth's interior: Analysis of the global data set, *Rev. Geophys.*, *31*, 267–280.

Stegman, D. R., A. M. Jellinek, S. A. Zatman, J. R. Baugardner, and M. A. Richards (2003), An early lunar core dynamo driven by thermo-chemical mantle convection, *Nature*, *421*, 143–146.

Tackley, P. J. (1997), Effects of phase transitions on three-dimensional mantle convection, in *The Fluid Mechanics of Astrophysics and Geophysics*, vol. 5, *The Doornbos Volume*, edited by D. Crossley, pp. 273–336, Gordon and Breach, New York.

Tackley, P. J. (1998), Three-dimensional simulations of mantle convection with a thermo-chemical basal boundary layer: D″?, in *The Core-Mantle Boundary Region*, *Geodyn. Ser.*, vol. 28, edited by M. Gurnis et al., pp. 231–253, AGU, Washington, D. C.

Tackley, P. J., and S. Xie (2003), STAG3D: A code for modeling thermo-chemical multiphase convection in Earth's mantle, paper presented at Second MIT Conference on Computational Fluid and Solid Mechanics, Cambridge, Mass.

Tackley, P. J., D. J. Stevenson, G. A. Glatzmaier, and G. Schubert (1994), Effects of multiple phase transitions in a three-dimensional spherical model of convection in Earth's mantle, *J. Geophys. Res.*, *99*(B8), 15,877–15,902.

Thomas, C., E. J. Garnero, and T. Lay (2004a), High-resolution imaging of lowermost mantle structure under the Cocos plate, *J. Geophys. Res.*, *109*, B08307, doi:10.1029/2004JB003013.

Thomas, C., J. Kendall, and J. Lowman (2004b), Lower-mantle seismic discontinuities and the thermal morphology of subducted slabs, *Earth Planet. Sci. Lett.*, *225*, 105–113.

Tozer, D. C. (1972), The present thermal state of the terrestrial planets, *Phys. Earth Planet. Inter.*, *6*, 182–197.

Tsuchiya, T., J. Tsuchiya, K. Umemoto, and R. M. Wentzcovitch (2004), Phase transition in $MgSiO_3$ perovskite in the Earth's lower mantle, *Earth Planet. Sci. Lett.*, *224*, 241–248.

van Keken, P. E. (2001), Cylindrical scaling for dynamical cooling model of the Earth, *Phys. Earth Planet. Inter.*, *124*, 119–130.

Weidner, D. J., and Y. Wang (1998), Chemical and Clapeyron-induced buoyancy at the 660 km discontinuity, *J. Geophys. Res.*, *103*, 7431–7441.

Xie, S., and P. J. Tackley (2004a), Evolution of helium and argon isotopes in a convecting mantle, *Phys. Earth Planet. Inter.*, *146*, 417–439.

Xie, S., and P. J. Tackley (2004b), Evolution of U-Pb and Sm-Nd systems in numerical models of mantle convection and plate tectonics, *J. Geophys. Res.*, *109*, B11204, doi:10.1029/2004JB003176.